

pubs.acs.org/JPCB Article

Csk α C Helix: A Computational Analysis of an Essential Region for Conformational Transitions

Published as part of The Journal of Physical Chemistry virtual special issue "Jose Onuchic Festschrift".

Raphael Vinicius Rodrigues Dias, Carolina Tatiani Alves Ferreira, Patricia Ann Jennings, Paul Charles Whitford, and Leandro Cristante de Oliveira*



Cite This: J. Phys. Chem. B 2022, 126, 10587-10596



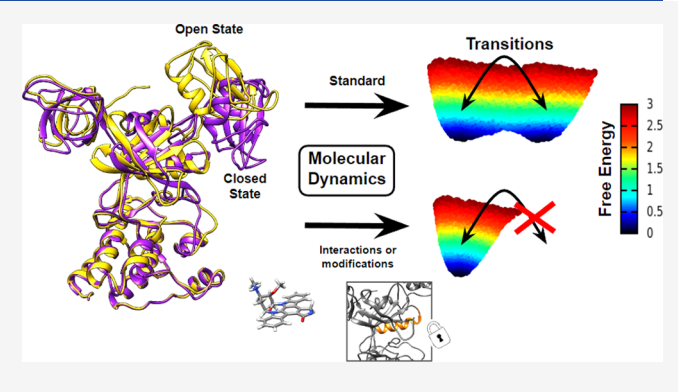
ACCESS

III Metrics & More

Article Recommendations

Supporting Information

ABSTRACT: Conformational changes are an essential feature for the function of some dynamic proteins. Understanding the mechanism of such motions may allow us to identify important properties, which may be directly related to the regulatory function of a protein. Also, this knowledge may be employed for a rational design of drugs that can shift the balance between active and inactive conformations, as well as affect the kinetics of the activation process. Here, the conformational changes in carboxylterminal Src kinase, the major catalytic repressor to the Src family of kinases, was investigated, and it was proposed as a functionally related hypothesis. A $C\alpha$ Structure-Based Model ($C\alpha$ -SBM) was applied to provide a description of the overall conformational landscape and further analysis complemented by detailed



molecular dynamics simulations. As a first approach to $C\alpha$ -SBM simulations, reversible transitions between active (closed) and inactive (open) forms were modeled as fluctuations between these two energetic basins. It was found that, in addition to the interdomain Carboxyl-terminal SRC Kinase (Csk) correlated motions, a conformational change in the α C helix is required for a complete conformational transition. The result reveals this as an important region of transition control and domain coordination. Restrictions in the α C helix region of the Csk protein were performed, and the analyses showed a direct correlation with the global conformational changes, with this location being propitious for future studies of ligands. Also, the Src Homology 3 (SH3) and SH3 plus Src Homology 2 (SH2) domains were excluded for a direct comparison with experimental results previously published. Simulations where the SH3 was deleted presented a reduction of the transitions during the simulations, while the SH3-SH2 deletion vanishes the Csk transitions, corroborating the experimental results mentioned and linking the conformational changes with the catalytic functionality of Csk. The study was complemented by the introduction of a known kinase inhibitor close to the Csk α C helix region where its consequences for the kinetic behavior and domain displacement of Csk were verified through detailed molecular dynamics. The findings describe the mechanisms involving the Csk α C helix for the transitions and also support the dynamic correlation between SH3 and SH2 domains against the Csk lobes and how local energetic restrictions or interactions in the Csk αC helix can play an important role for long-range motions. The results also allow speculation if the Csk activity is restricted to one specific conformation or a consequence of a state transition, this point being a target for future studies. However, the α C helix is revealed as a potential region for rational drug design.

INTRODUCTION

Conformational changes are an important feature of some regulatory proteins and molecular motors, playing an essential role in living cells. The comprehension of the mechanisms involved in this process has allowed the understanding of several biological processes. ^{1–3} One interesting target for these studies is the Carboxyl-terminal SRC Kinase (Csk), a catalytic repressor responsible for phosphorylation, cell-growth control, and differentiation, being the main down regulator of Src Family Kinases (SFKs). ^{4–7} The proper functioning of Csk is crucial to cell health, as illustrated by the fact that the loss of function of

Csk leads to constitutive activation of SFKs, accompanied by defects in embryonic development.⁸ On the other hand, the gain of function of Csk can readily downregulate SFK-mediated cell

Received: July 30, 2022 Revised: November 22, 2022 Published: December 13, 2022





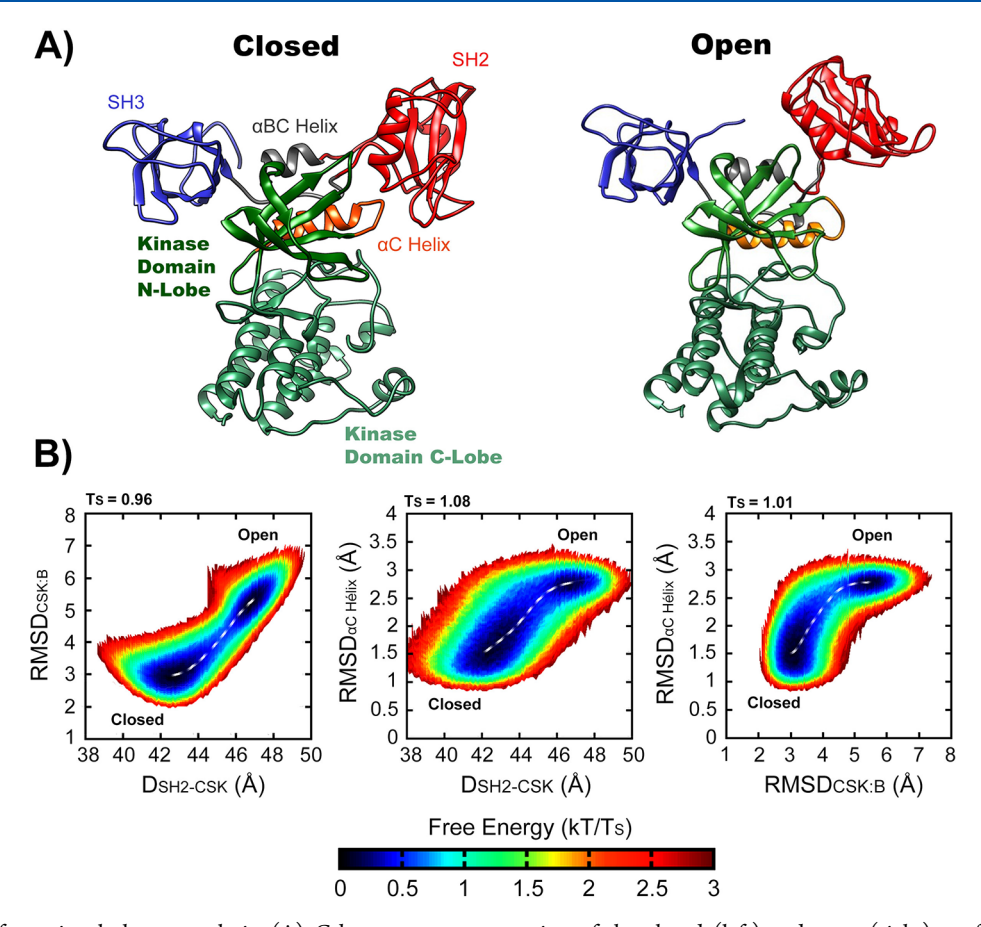


Figure 1. Csk conformational change analysis. (A) Csk cartoon representation of the closed (left) and open (right) conformations from the crystallographic structure (PDB ID: 1K9A, chains B and C, respectively), colored in order to highlight domains and specificity. SH3, SH3–SH2 linker, SH2, α C helix, small kinase lobe (N-Lobe), and large kinase lobe (C-Lobe) are in blue, gray, red, orange, green bean, and green forest, respectively. (B) Free energy surface of Csk calculated from $C\alpha$ -SBM simulations using three different reaction coordinates: distance between the SH2 domain and C-terminal Lobe Kinase ($D_{SH2-CSK}$), Root Mean Square Deviation for the full structure (RMSD_{CSK:B}), and RMSD of the Csk α C helix (RMSD_{αCHelix}), both RMSDs using the chain B (closed form) as reference. The free energy values follow the colorbar scale presented below from 0 (black) to 3 (dark red) normalized by the transition state temperature (T_S). The dashed line represents the lowest energy path between the two minimums.

signaling, which results in pathological consequences such as colon cancer. 9

Csk is a 450-residue protein composed of four domains: Src Homology 2 (SH2), Src Homology 3 (SH3), and kinase small (Csk N-Lobe) and kinase large (Csk C-Lobe) lobes. The X-ray crystallographic structure (2.5 Å resolution) presents 6 chains where 2 of them (chains C and D) are highlighted for the more distant positioning of the SH2 domain, among other differences, assumed as inactive (open form), and 4 more compact ones (chains A, B, E, and F) are considered as active (closed form), identified in the Protein Data Bank by the code 1K9A. ¹⁰

However, small-angle X-ray scattering analysis revealed a dynamic equilibrium between representative ensembles of conformations more extended and collapsed in solution¹¹ that can be shifted in the presence of ligands such as adenylyl imidodiphosphate (AMP-PNP), a nonhydrolyzable analogue of adenosine 5'-triphosphate (ATP) and adenosine 5'-diphosphate (ADP).¹²

All four domains have been shown to be required for the proper function of Csk, ^{10,13-16} though the atomistic understanding of the role of each domain on the global function is not fully understood. In many tyrosine protein kinases, the balance between active and inactive conformations is largely affected by the phosphorylation state of the C-terminal tyrosine tail, ¹⁷

presumably by directly stabilizing a particular relative positioning of the domains.

Figure 1A shows a cartoon illustration of the open and closed Csk forms based on the crystallographic structure, identifying domains and important local regions. When compared with other Src Family members, Csk lacks a C-terminal phosphorylation site and activation/inactivation is often induced by cofactor interactions that are distal to the active site and do not appear to induce large-scale domain rearrangements. Accordingly, Csk must possess some form of internal communication channels between these distal sites and the ATP-binding site through modest shifts in either local configuration or dynamics.

Due to the biological importance of Csk, many studies have focused on exploring the interplay between the various domains of Csk and catalytic activity. 14,15,20–23 These studies have indicated important regions and residues that appear to be coupled to the functional properties of Csk. The importance of the noncatalytic domains (SH2 and SH3) is evidenced, for example, in domain deletion studies, which show the kinase activity reduced by 70% and 96% with the deletion of SH3 and SH2, respectively. 14,18,24 Still, the mutation of SER78, which is found in the SH2 domain, to Asp results in a reduction of the activity by more than 90% 14 under certain chemical scenarios.

Some experiments using the deuterium incorporation tax to the wild-type and PHE183 mutants¹⁵ reveal that α C helix and SH2-kinase linker are components that regulate the conformational change by the modulation between the SH2 domain and kinase domain. The same technique was applied to investigate the activation by CBP peptide, which increases the catalytic activity and suggests a mechanism of regulation. 15 NMR spectra obtained from oxidized and reduced forms of the SH2 domain showed that a particular disulfide bond can decrease the catalytic activity when formed, explained by the increasing strain around the binding site region and α C helix in SH2.²⁵ For all cases, normal-mode analysis showed how the flexibility of different regions is affected by mutations or CBP binding. 15 Despite this set of results showing the importance of communication between all domains present in Csk, a detailed description of these mechanisms can be exploited through computational evaluations, identifying the importance of specific regions for conformational changes in Csk and the development of new products, for example, the rational drug design for desirable features.

METHODS

Cα Structure-Based Model and Dual Basin Construc-

tion. Since the identification of essential elements for the mechanism's comprehension of conformational changes in Csk is desired, the $C\alpha$ Structure-Based Model ($C\alpha$ -SBM) is a suitable approach for the study. SBMs are versatile because they allow efficient conformational searching and as a consequence the employment of statistical mechanics for the analysis. They have been used for several purposes as the prospection of protein mechanisms, $^{26-28}$ conformational transitions, 1,29 or structural characterization when combined with experimental data 11,12,30,31

In this study, protein amino acids are represented by rigid spheres centered on the α carbon position.³² The potential energy of the system is based on the geometrical characteristics of the native structure (Γ_0) compared to the current conformation (Γ) throughout the molecular dynamics simulation and given by

$$\begin{split} V(\Gamma, \, \Gamma_{\!\scriptscriptstyle o}) &= \sum_{\text{bonds}} \, \varepsilon_{\!\scriptscriptstyle r} (r - r_{\!\scriptscriptstyle o})^2 \, + \sum_{\text{angles}} \, \varepsilon_{\!\scriptscriptstyle \theta} (\theta - \theta_{\!\scriptscriptstyle o})^2 \\ &+ \sum_{\text{backbone}} \, \varepsilon_{\!\scriptscriptstyle \phi} \bigg\{ \left[1 \, - \, \cos(\phi - \phi_{\!\scriptscriptstyle o}) \right] \\ &+ \frac{1}{2} [1 \, - \, \cos(3(\phi - \phi_{\!\scriptscriptstyle o}))] \bigg\} \, + \sum_{\text{contacts}} \, \varepsilon_{\!\scriptscriptstyle C} \bigg[5 \bigg(\frac{d_{ij}}{r_{ij}} \bigg)^{12} \\ &- 6 \bigg(\frac{d_{ij}}{r_{ij}} \bigg)^{10} \bigg] \, + \sum_{\text{non-contacts}} \, \varepsilon_{\!\scriptscriptstyle NC} \bigg(\frac{\sigma_{\!\scriptscriptstyle NC}}{r_{ij}} \bigg)^{12} \end{split}$$

where r_{ij} is the distance between atom i and j and d_{ij} represents the distance between i and j in which the interaction energy is minimum. The instantaneous bond lengths, bond angles, and dihedral angles are given by r, θ , and ϕ , respectively, and r_0 , θ_0 , and ϕ_0 are the corresponding values in the native structure. The energetic prefactors used were: $\epsilon_r = 100 \ \epsilon_C$, $\epsilon_\theta = 20 \ \epsilon C$, and $\epsilon_\phi = \epsilon_{\rm NC} = \epsilon_C$, where ϵ_C is equal to 1 unit (in reduced units) with contact interaction pairs defined by the Shadow Contact Map algorithm.³³ Structure-based models, in general, are widely

employed for the study of protein mechanisms, and they are detailed in several references. ^{28,32,34}

The crystallographic configurations¹⁰ and Small Angle X-ray Scattering analysis of Csk in solution^{11,12} suggest the energy landscape of Csk does not have a single well, being composed of at least two basins. Since the inactive form (open) is highly degenerate and the main target is to reach the active form (closed) through conformational transitions, the use of the forms present in the crystal structure is acceptable. Thus, the evaluation of conformational changes involved the chains B and C, the closed and open forms, respectively, from the Csk crystal structure (PDB ID: 1K9A), where missing residues were added using PROFIX.³⁵ However, individual dynamics of each chain potential [eq 1] are unable to access the other state; i.e., $C\alpha$ -SBM molecular dynamics of chain B does not access the native structure of C and vice versa in any temperature (see Figure S3). Therefore, a hybrid potential (aka Dual-Gö) was constructed following the procedures employed by Whitford et al., combining the contacts of both conformations in a unique contact map. Exclusive contact pairs in closed form with distances 50% greater than in the open structure are selected and included in the open structure contact map, allowing by a finetuning the evaluation of conformational transitions between both forms. Consequently, the energy prefactors of the contacts $(\epsilon_{\rm C})$ added are multiplied by a constant $(2.1 \times \epsilon_{\rm C})$, setting up the system for the conformational changes at an adequate range of temperatures between glass $(T_{\rm g})$ and unfolding $(T_{\rm u})$ (details in Figure S4). The energy function construction method assumes that these unique contacts selected from the closed form are responsible to drive the open conformation to the closed through the fine-tuning of the energetic prefactor. Nevertheless, it is important to mention that this approach requires conformations similar enough to have the essential contacts that drive one form to another present. Simulations where SH3 or SH2-SH3 domains were deleted employed this same adjusted potential, preserving only the applicable force field for the remaining residues.

Setup for SBM Simulations and Mimetic Construction of Inhibitors. The input files for SBM were generated by the SMOG web server³⁶ and modified when needed (see $C\alpha$ Structure-Based Model and Dual Basin Construction). Molecular dynamics (MD) simulations were performed using GROMACS 4.5.7^{37,38} where a temperature bath was coupled by Langevin Dynamics with a constant equal to 1 ps, as implemented elsewhere.³⁴ Simulations to evaluate conformational changes started with the protein in its open conformation in a total of 5×10^9 steps for each temperature evaluated and using a time step of 0.0005 time units. The configurations and energies were recorded every 5000 steps. Three different reaction coordinates were used to follow the conformational transitions between the two states: Distance between the SH2 and C-terminal Lobe Kinase domains ($D_{SH2-CSK}$), RMSD of the complete protein using the native structure in the closed form as a reference (RMSD_{CSK:B}), and RMSD of the α c helix located in the N-terminal Lobe Kinase (RMSD $_{\alpha C \text{ helix}}$), also using as reference structure the closed form. The closed conformation (PBD ID: 1K9A:B) is given as the Csk active form; ¹⁰ thereby, it was chosen as a reference for comparative purposes (dihedral angles and RMSD values). The analyses were performed using a GROMACS provided tool, and the free energy profiles were calculated through the Weighted Histogram Analysis Method (WHAM).³⁹ The WHAM package was obtained from SMOG web server and for the calculations used 300 bins for each input

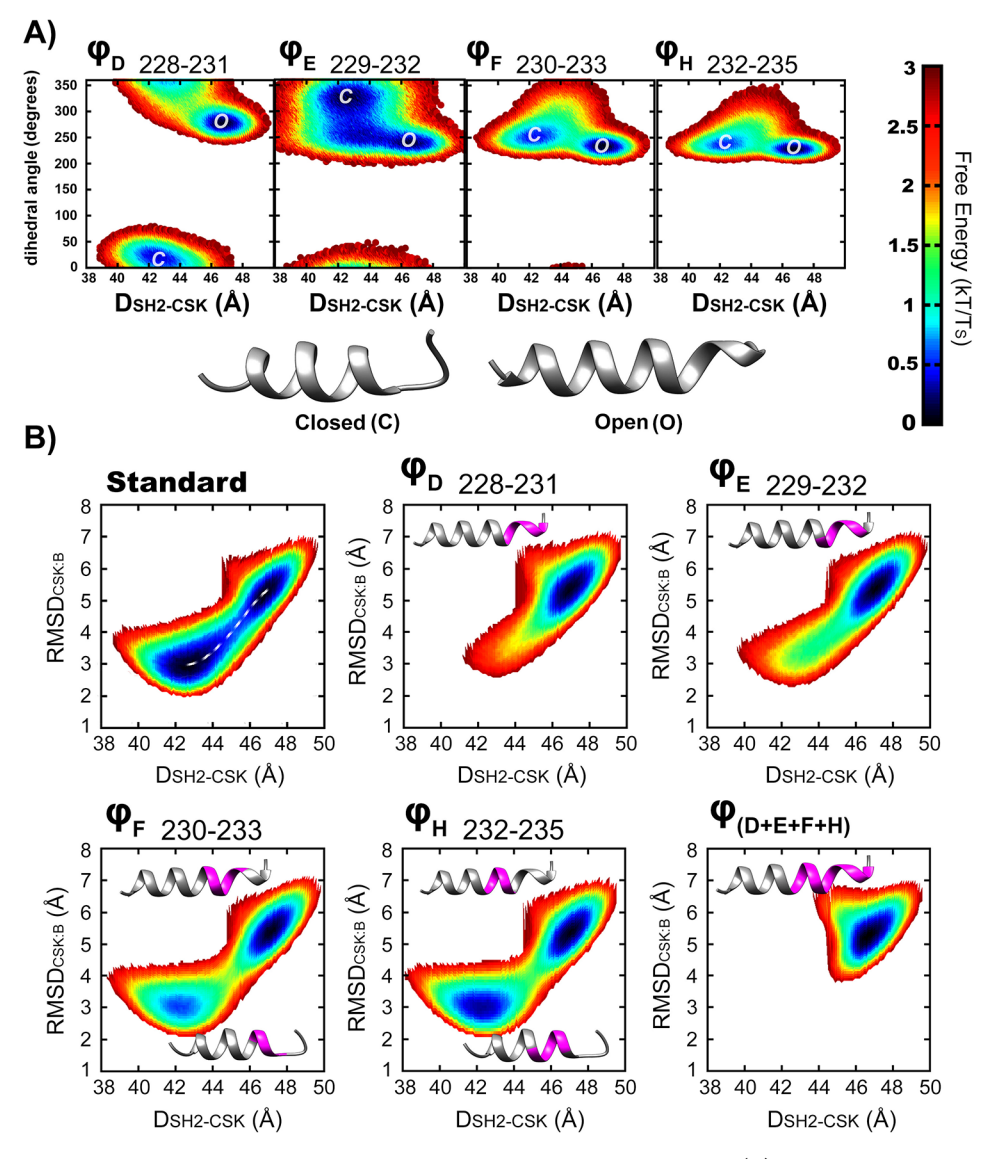


Figure 2. Effect of conformational changes under the viewpoint of Csk α C helix dihedral angles. (A) Free energy surfaces using the specifically indicated dihedral angles as reaction coordinates. (B) Influence of angular restrictions in located α C helix regions. The label "standard" is a free energy surface reference where dihedral angular restrictions were not imposed, followed by the specifically hardened angles. Disturbed dihedrals via an increase of pre-energy factors were highlighted in the cartoon representation in purple.

and a tolerance for the convergence of 1×10^{-3} in free energy variation.

The Csk—Staurosporine complex was constructed based on the crystallographic information available at PDB using the identification code 3D7T, 40 chain A (reinforced by PDB ID: 1QPJ, lymphocyte-specific protein tyrosine kinase (Lck) in complex with staurosporine), that lacks the SH2 and SH3 domains, through STAMP structural alignment 41 with the Csk structure (PDB ID: 1K9A). The staurosporine (STU) interaction effect is introduced implicitly using a harmonic potential $\left(\frac{1}{2}\times \epsilon_{\rm C}\times (r-r_0)^2\right)$ where the residues i and j are determined by the distance from the residues to the inhibitor. If two residues are up to 6 Å apart from the same atom of the staurosporine, then they are considered interacting in the mimetic potential.

Detailed Molecular Dynamics Simulations. MD simulations using explicit water and ions were performed to evaluate the consistence of the mimetic construction of the inhibitor and complement the analysis with an inhibitor. These detailed MD

simulations were performed with GROMACS 4.5.7 using CHARMM27 force field⁴² with the standard setup for the protein residues and TIP3P water model. The ligand parametrization was calculated using the Web server Swiss-param from the Swiss Institute of Bioinformatics. 43 The MD minimization was done using 50000 steepest-descent steps and 5000 conjugate gradient steps, both without position restraints. The equilibration was performed in two steps with 100 ps, initially with and then followed without position restrictions for the protein and ligand atoms, when applicable. Initial atom velocities were based on the Maxwell-Boltzmann distribution and the MD simulations for 100 ns with an integration step of 2 fs at 300 K, salt concentration of 0.15 M for the net neutralization, and 1 atm. The trajectory positions and energies were recorded every 100 ps. The simulation used Parrinello-Rahman barostat, 44 Berendsen thermostat, 45 and LYNCS method to constrain all hydrogen bonds⁴⁶ and a simulation box built with the edges of the box with 10 Å from the

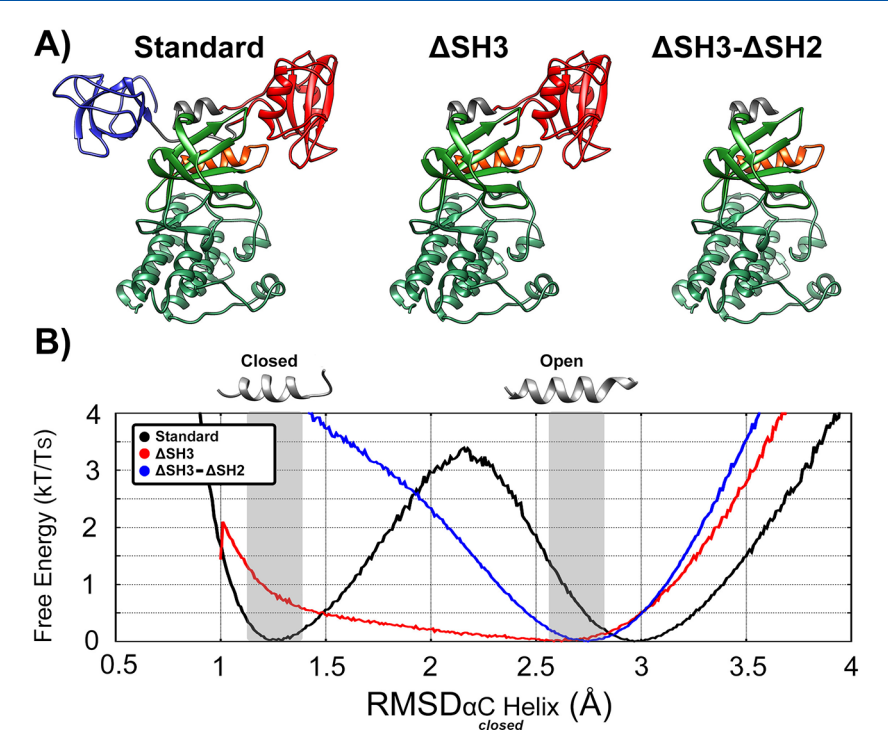


Figure 3. Effects of SH3 and SH3–SH2 domain deletions. (A) Cartoon representations of Csk tridimensional structure (left), Csk without SH3 domain (center), and Csk without SH3–SH2 domains (right), labeled by standard, Δ SH3, and Δ SH3– Δ SH2, respectively. (B) Free energy profiles based on the RMSD_{α C helix} (chain B as reference) reaction coordinate to standard, Δ SH3, and Δ SH3– Δ SH2.

protein surface and periodic boundary conditions. MD analyses were done using tools available in the GROMACS package.

RESULTS

Evaluation of Conformational Changes through Structure-Based Model Simulations. Previous studies have emphasized the importance of the Csk α C helix;⁴⁷ thus, initially, the C α -SBM accuracy was evaluated to capture this feature. The free energy surfaces using $C\alpha$ -SBM simulations with dual-conformational potential (hybrid potential) are presented in Figure 1B, where different reaction coordinates were employed, the distance between the SH2 domain and Cterminal Lobe Kinase ($D_{SH2-CSK}$), Csk RMSD (RMSD_{CSK:B}), and Csk α C helix RMSD (RMSD $_{\alpha$ C helix), where these last two parameters are related to the closed form (CSK:B). The analysis of these profiles reinforce how large movements, as described by the reaction coordinates $D_{SH2-CSK}$ and RMSD_{CSK:B}, are related to localized regions as the Csk α C helix. The free energy profiles under a unique coordinate reaction are also available in Figure S1 for viewing and quantification purposes.

Extensive searching of essential regions for functional transition control was performed for the simulations (data not shown). The analysis indicated the α C helix as the most promising region, where a detailed evaluation is presented in Figure 2A. The α C helix consists of 19 residues (from 225 to 243) that were divided into 16 dihedrals angles for calculation purposes. Each dihedral angle was used as a reaction coordinate to evaluate how specific residues are correlated with the $D_{\rm SH2-CSK}$ values during the simulations. Since the relationship between the global coordinate reactions (RMSD_{CSK:B} and $D_{\rm SH2-CSK}$) and local values (RMSD $_{\alpha \rm C \ helix}$ and dihedral angles) was verified, as presented in Figures 1B and 2A, this consideration as an indirect coordinate reaction is suitable. The dihedral angles were sequentially labeled $\phi_{\rm A}$, $\phi_{\rm B}$, ..., and $\phi_{\rm P}$,

corresponding to angles formed by the residues 225–228, 226–229, ..., and 240–243. Among the 16 dihedrals analyzed (see Figure S2), four of them had a considerable barrier in the transition state on Csk conformational transitions, corresponding to the angles ϕ_D , ϕ_E , ϕ_F , and ϕ_H formed by the residues 228–231, 229–232, 230–233, and 232–235, respectively, detached in Figure 2A. The first two mentioned angles, ϕ_D and ϕ_E , have distinct values to the open and closed states properly characterizing these forms, while the two others, ϕ_F and ϕ_H , have basins with close values. Here, these close angular values can be understood as thermal fluctuations not effectively acting as a control region for conformational transitions. Thus, this small region involving ϕ_D and ϕ_E undergoes a high strain energy during the transitions and can work as a trigger for the shift between the open and closed states.

To evaluate the hypothesis of the Csk α C helix works as a region of control, an increase in the energetic prefactor of these dihedrals $(5 \times \epsilon \phi)$ was made in order to stiffen the four dihedral torsions and probe their impact on the conformational changes. In Figure 2B, the free energy surfaces for the case using RMSD_{α C helix} versus $D_{SH2-CSK}$ are presented. Since the interference imposed in the dihedral angles affects its usage as a reaction coordinate for the analysis, a new one was employed. From the results, it is possible to note that the restriction imposed to the angles $\phi_{\rm E}$, $\phi_{\rm E}$, and $\phi_{\rm H}$ solely is unfavorable for the conformational transitions by the increase of the transition state barrier. With the restriction imposed to ϕ_{D} exclusively, transitions become more limited, and when all of them $(\phi_{
m D},$ $\phi_{\rm E}$, $\phi_{\rm F}$ and $\phi_{\rm H}$) are restricted, they just do not occur. It is important to clarify that nonequal populations of the basin in these profiles are due to the protein starting to unfold with the increase of the temperature without reaching the fullness of the transitions between the basins.

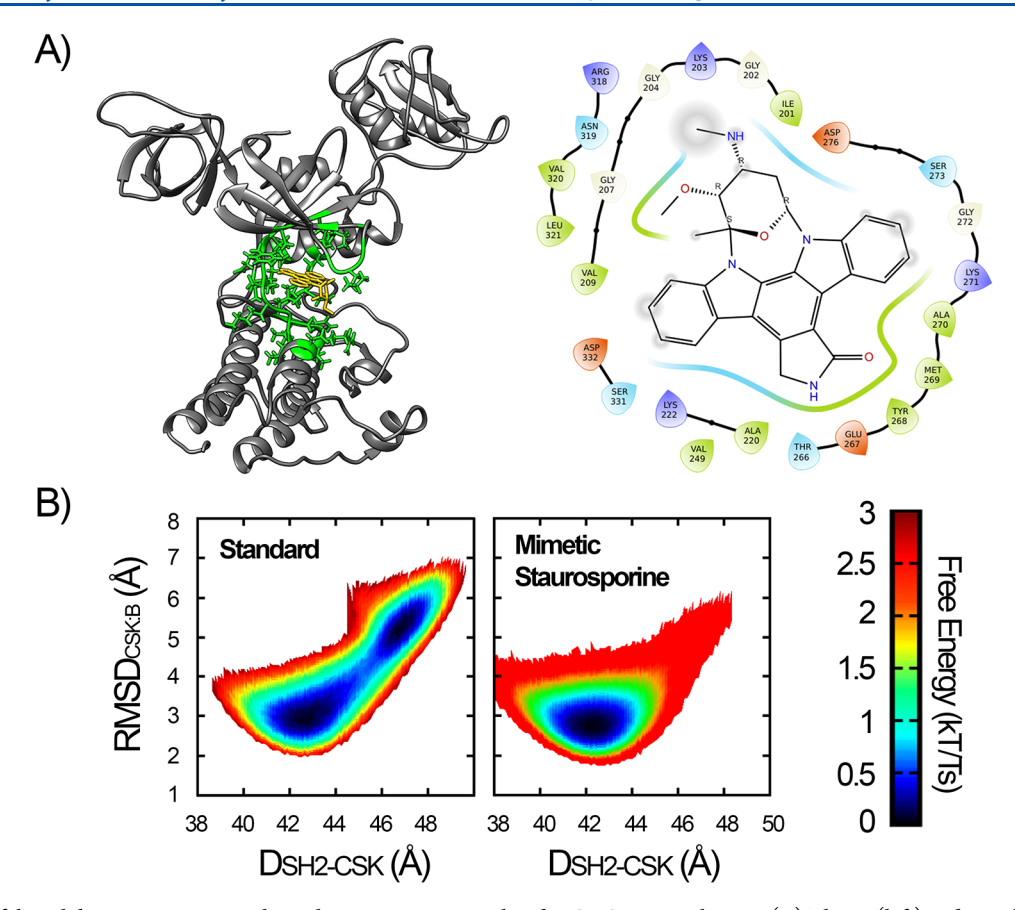


Figure 4. Effect of the inhibitor staurosporine through a mimetic potential under $C\alpha$ -SBM simulations. (A) Three- (left) and two-dimensional (right) representation of staurosporine interactions with Csk. Residues highlighted in green in the cartoon are at a distance up to 6 Å from the ligand, presented in yellow. The 2D map of the interactions was generated using Maestro (Schrödinger Release 2022-2: Maestro, Schrödinger, LLC, New York, NY, 2021) where hydrophobic residues are in green, positively charged residues are in blue, negatively charged residues are in red, and apolar residues are in cyan. The gray atomic background represents the solvent-accessible surface area (SASA) of the atom. (B) Free energy surfaces for the $C\alpha$ -SBM simulations with the dual potential without modifications (left) and mimetizing the staurosporine bound.

In summary, each of these highlighted dihedrals directly affects conformational transitions by increasing the energy barrier between the two states. Consequently, when all are stressed simultaneously, the transitions stop completely, making Csk stay predominantly in just one state during molecular dynamics simulations. Also, the obtained energetic profiles reinforce the relationship between global and local movements and the SH2 and SH3 modulation, indicating that the α C helix is a promising region for further studies, which also goes through conformational variations during the transition.

Effects of Domain Deletion for the Conformational Transitions. The importance of SH3 and SH2 coordination^{23,48} and influence on the Csk activity¹⁵ were explored by the removal of these domains. Computational simulations were performed through C α -SBM molecular dynamics with the deletions of SH3 (Δ SH3) and SH3-SH2 (Δ SH3- Δ SH2) domains, as represented by cartoons in Figure 3A. Based on the free energy profiles shown in Figure 3B, using $D_{SH2-CSK}$, it is noted that the absence of the SH3 domain destabilizes the dynamic coupling between the domains and by consequence the correlated movement of SH2 and α C helix. Yet, SH2 has a displacement more restricted to a $D_{SH2-CSK}$ around 43 Å, where previously the typical values were 42 and 47 Å, relative to the closed and open forms, respectively. Such behavior, keeping the SH2 domain in a position closer to the closed conformation after the SH3 deletion, raises the speculation that the functional

activity may be related to the overall movement of Csk and not limited to a specific state, which should be the subject of investigation in future works. Thus, deletion of the SH3 domain partially affected the conformational transition of Csk decreasing the number of conformational transitions.

The deletion of the SH3 and SH2 domains together vanishes the transitions, with RMSD $_{\alpha \text{C helix}}$ becoming uncoordinated with the well values around the closed form basin.

Effect of a Kinase Inhibitor for the Transitional Changes: A Starting Point for the Rational Design of **New Drugs.** Another interesting point is to understand how an inhibitor affects the mechanisms related to Csk conformational transitions by its proximity to the αC helix residues and restraints imposed by the molecular interactions. Thus, staurosporine (STU), a known inhibitor among Csk-like protein kinases, 40,50 was chosen for the evaluation, mainly due to the availability of a crystallographic structure (PDB ID: 3D7T). Initially, the results of $C\alpha$ -SBM with the mimetic complexed potential (see Methods) were compared with the noncomplexed (standard) dual basin potential. Figure 4A shows Csk complexed with staurosporine (left) represented by a cartoon and the residues highlighted with sticks that were used to build the mimetic potential (right). Figure 4B shows the free energy surface using $D_{\rm SH2-CSK}$ and ${\rm RMSD_{CSK:B}}$ as reaction coordinates, indicating an ensemble limited to the closed form to the mimetic potential. Of course, the closed form is populated due to the way

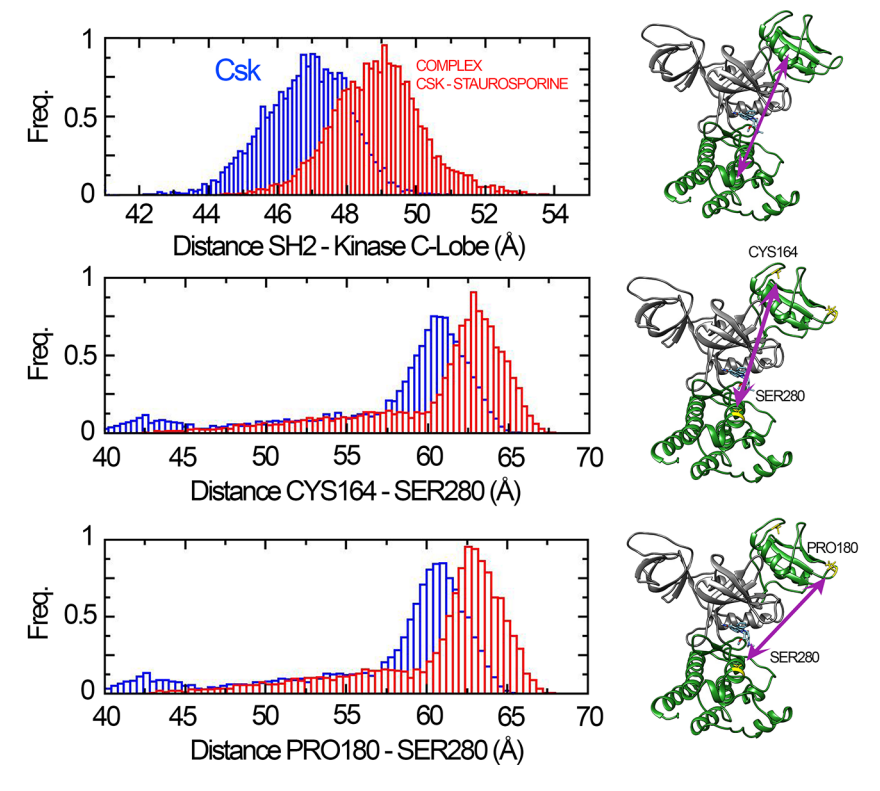


Figure 5. Detailed molecular dynamics simulations of Apo Csk and complexed with staurosporine. The histograms on the left show distributions of distance (distances between the center of mass of the SH2 domain and C-terminal Lobe Kinase, CYS164 and SER280, and PRO180 and SER280) to the Apo Csk (blue) and CSK—Staurosporine complex (red) obtained from simulations with a respective cartoon representation on the right. Purple double arrows highlight the distances involved with sparse residues in yellow.

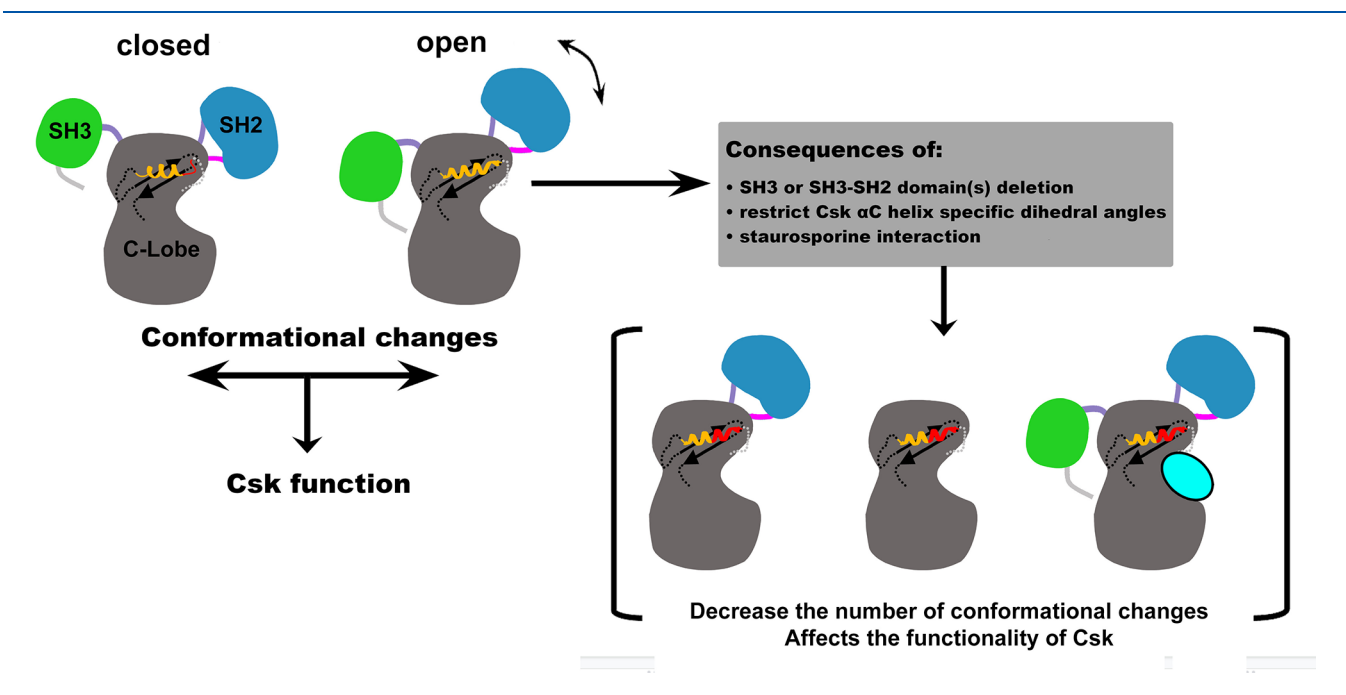


Figure 6. Summary of the elements that affect Csk conformations transitions directly related to the α C helix.

the dual potential is constructed. However, the mimetic potential practically vanishes the transitions between the two basins. Again, the understanding is that STU affects the transitions and as a consequence the Csk activity.

Since the closed form is understood as being active and its population obtained from $C\alpha$ -SBM for the mimetic potential can be an artifact of the construction, detailed molecular

dynamics simulations with explicit atoms using GROMACS were performed to evaluated Csk without any ligand and complexed with staurosporine. It is known that these molecular dynamics do not allow conformational changes as calculated using SBM; in contrast, they allow one to verify the influence of the ligand for structural stabilization of the complex, small movements including side chains and residue fluctuations.

The detailed molecular dynamics simulations indicated a stable complex. The evaluation of the regime of residue fluctuations did not show significant variations for both cases (Figure S5). However, the analysis of the trajectories with and without the STU inhibitor revealed different distance distributions under different parameters. Assuming the histogram distributions in Figure 5, calculated using the distances between the centers of mass SH2 and C-terminal Kinase (top), CYS164-SER280 (middle), and PRO180-SER280 (bottom), note that Csk may have some structural movements which do not occur in the dynamics of the complex, based on the peaks despite the similar widths. The complex shows a profile with values of these chosen parameters, for example, the peaks to distances between the centers of mass SH2 and C-terminal Kinase being 47 and 49 Å to noncomplexed and complexed states, respectively. Here, it is evident that for both, $C\alpha$ -SBM and detailed molecular dynamics simulations, the main effect of staurosporine in Csk in conformational terms is to prevent large movements of the SH2 domain, making the transitions between open and closed states difficult to occur in complexed Csk (holo) than in Apo. A summary of the elements that affect the Csk conformational transitions directly related to the αC helix region is presented in Figure 6.

DISCUSSION

Although having structural similarity to other SFK members, Csk differs in its structural arrangement and functioning mechanism. 11,40 For SFKs, the catalytic activity is negatively modulated by interactions between a phosphorylated Cterminal tail and the SH2 domain.⁴ These interactions can be reversed by other proteins such as Cbp/PAG phosphatase that dephosphorylate the C-terminal tail and undo the interaction. Csk lacks this phosphorylated C-terminal tail and as consequence presents a regulatory mechanism different from the other SKFs. Thereby, Csk conformational changes are strongly related to the modulation between its domains, including specific regions. The results shown here indicate that αC helix is an essential region for these functional transitions since it establishes a coordination between the Csk domains and acts as a controlling region where local conformational changes are directly related to global conformational changes. This feature provides a considerable potential for the rational design of inhibitors with more competitive costs than STU, especially if the interaction mechanism is able to restrict the degree of freedom of the Csk α C helix. The importance of this region has already been reported by several authors; 47,49 however, the association of the restrictions in the α C helix as a result of the inhibitor interaction pushes forward the knowledge about how this small region works as a trigger for the Csk conformational change and by consequence on its activity. Still, it is important to highlight that the computational simulations employed do not evaluate the activity properly; i.e., this is only an indirect hypothesis associated with the conformational transitions or the possibility of the active (closed) form to be reached.

Following the same reasoning, the study of the role of an inhibitor (STU) by an additional layer of sophistication brought by the detailed molecular dynamics simulations supported the evidence pointed by the simple $C\alpha$ -SBM mimetic construction and the stiffening of dihedral angles along the α C helix specific residues, in terms of making the transitions more difficult in the presence of STU. Still, when the detailed molecular dynamics simulations were explored, a higher distance from the SH2

domain and the kinase lobes was found, which in some way corroborates with the Jamros et al. SAXS characterization where conformational shift effects were found in other Csk interactors. In the mentioned study, the Apo Csk, AMP-PNP (an analog of the ATP) bound Csk, and the ADP bound Csk showed different sets of 3 prominent conformational populations, varying the radius of gyration from lower values for Apo Csk to higher values for ADP bound Csk. This result corroborates with that presented in Figure 5 where the Apo Csk shows lower distances between the SH2 domain and the Csk C-Lobe center of mass than those in the Csk—Staurosporine complex, since in this case, the radius of gyration and SH2-Csk C-Lobe distance are correlated. The analysis also suggests that the interaction of different molecules with the Csk α C helix may be the main reason for allosteric regulation.

Still, the comparison of the $C\alpha$ -SBM simulations employing the complete Csk and considering SH3 and SH2-SH3 domain deletions also corroborate with the experimental findings previously reported, 14,18,22,24 the activity values of 70% and 96%, respectively. Initially, it was possible to verify how important the coordination of SH2 and SH3 domains is with the α C helix and the Csk lobes, since the deletion results in a wilder representative ensemble without a clear population of two basins when evaluated under the $RMSD_{\alpha C \; helix:B}$ parameter, and related to a reduction of the Csk activity in experimental reports. These results can assume at least two hypotheses to relate computational simulations to the Csk activity, reserving the limitations of the modeling: (I) the Csk becomes less active due to staying a shorter time in the closed form, considered the active state, since the number of transitions decreases compared to the complete Csk; (II) the action of the Csk, as a molecular motor, occurs during the conformational transition, like scissors only cut when their blades are moving, in a naive comparison. The results discussed in this work allow even more speculations about how Csk conformational transitions in itself are related with movements where transitional states may be responsible for its regulation mechanism, these hypotheses being the subject of future work combining theoretical and experimental techniques.

CONCLUSIONS

The current work reinforces some previous results about the importance of the Csk α C helix region for the global Csk conformational transitions. By using $C\alpha$ -SBM, a dual-basin potential was constructed allowing the evaluation of conformational transitions between the Csk open and closed forms, based on the X-ray crystallography (PDB ID: 1K9A:B and 1K9A:C, respectively). Also, the introduction of restrictions in some αC helix dihedral angles, deletions of SH3 and SH2-SH3 domains, and construction of an inhibitor mimetic potential indicated how these perturbations affect the conformational transitions, in some cases vanishing them. Detailed molecular simulations were employed as an additional technique to explore the relationship between Csk elongation degree as a consequence of staurosporine interaction, a known inhibitor. This analysis still opens possibilities for new approaches and investigations, like drug rational design based on the variations in Csk α C helix as an indicator of conformational changes. Finally, the results corroborate with experimental evaluations previously reported by different authors, expanding the knowledge involving Csk mechanisms.

ASSOCIATED CONTENT

Supporting Information

The Supporting Information is available free of charge at https://pubs.acs.org/doi/10.1021/acs.jpcb.2c05408.

Free energy profiles under a unique coordinate reaction to $C\alpha$ -SBM dual potential, analysis of the dihedral angle torsions of the Csk α C helix during $C\alpha$ -SBM simulations using dual potential, absence of conformational transitions using nonmodified $C\alpha$ -SBM potentials, detailing of the $C\alpha$ -SBM dual potential construction, and analysis of residue deviation, fluctuation in explicit water and ions all-atoms MD simulations, and free energy profiles using all-atoms SBM simulations (PDF)

AUTHOR INFORMATION

Corresponding Author

Leandro Cristante de Oliveira — São Paulo State University (Unesp), Department of Physics, Institute of Biosciences, Humanities and Exact Sciences, São José do Rio Preto, São Paulo 15054-000, Brazil; ⊚ orcid.org/0000-0002-6932-6792; Phone: +55 (17)3221-2200; Email: leandro.cristante@unesp.br

Authors

Raphael Vinicius Rodrigues Dias — São Paulo State University (Unesp), Department of Physics, Institute of Biosciences, Humanities and Exact Sciences, São José do Rio Preto, São Paulo 15054-000, Brazil

Carolina Tatiani Alves Ferreira — São Paulo State University (Unesp), Department of Physics, Institute of Biosciences, Humanities and Exact Sciences, São José do Rio Preto, São Paulo 15054-000, Brazil

Patricia Ann Jennings — University of California, San Diego, La Jolla, California 92093, United States; orcid.org/0000-0002-7478-2223

Paul Charles Whitford — Northeastern University, Department of Physics and Center for Theoretical Biological Physics, Boston, Massachusetts 02115, United States; ◎ orcid.org/0000-0001-7104-2265

Complete contact information is available at: https://pubs.acs.org/10.1021/acs.jpcb.2c05408

Notes

The authors declare no competing financial interest.

ACKNOWLEDGMENTS

We would like to thank Professor José Nelson Onuchic for the discussions about the Csk conformational transitions and support and Professor Fernando Alves de Melo for the discussions about the SH3 and SH2 domains and their role in protein kinases. R.V.R.D. would like to thank FAPESP and CAPES and C.T.A.F. would like to thank CAPES for the scholarships. This research was supported by grants from Conselho Nacional de Desenvolvimento Científico e Tecnológico - CNPq 442352/2014-0 and Fundação de Amparo à Pesquisa do Estado de São Paulo - FAPESP grant no. 2016/ 08753-6. P.C.W. was supported by NSF grant MCB-1915843. Work at the Center for Theoretical Biological Physics was also supported by the NSF (Grant PHY-2019745). The simulations were performed at the Center for Scientific Computing (NCC/ GridUNESP) of the São Paulo State University (UNESP) and CENAPAD-SP (Centro Nacional de Processamento de Alto

Desempenho em Sao Paulo), project UNICAMP/FINEP-MCTII. Molecular graphics were performed with UCSF Chimera, developed by the Resource for Biocomputing, Visualization, and Informatics at the University of California, San Francisco, with support from NIH P41-GM103311. We would like to thank the anonymous reviewers for their helpful comments.

REFERENCES

- (1) Whitford, P. C.; Miyashita, O.; Levy, Y.; Onuchic, J. N. Conformational transitions of adenylate kinase: switching by cracking. *J. Mol. Biol.* **2007**, *366*, 1661–71.
- (2) Lopez, E. D.; Burastero, O.; Arcon, J. P.; Defelipe, L. A.; Ahn, N. G.; Marti, M. A.; Turjanski, A. G. Kinase Activation by Small Conformational Changes. *J. Chem. Inf. Model* **2020**, *60*, 821–832.
- (3) Orellana, L. Large-Scale Conformational Changes and Protein Function: Breaking the in silico Barrier. Front. Mol. Biosci. 2019, 6, 117.
- (4) Okada, M. Regulation of the Src family kinases by Csk. *Int. J. Biol. Sci.* **2012**, *8*, 1385–1397.
- (5) Thomas, S. M.; Brugge, J. S. Cellular functions regulated by SRC family kinases. *Annu. Rev. Cell Dev. Biol.* **1997**, *13*, 513–609.
- (6) Kawabuchi, M.; Satomi, Y.; Takao, T.; Shimonishi, Y.; Nada, S.; Nagal, K.; Tarakhovsky, A.; Okada, M. Transmembrane phosphoprotein Cbp regulates the activities of Src-family tyrosine kinases. *Nature* **2000**, *404*, 999–1003.
- (7) Brdička, T.; et al. Phosphoprotein associated with glycosphingolipid-enriched microdomains (PAG), a novel ubiquitously expressed transmembrane adaptor protein, binds the protein tyrosine kinase Csk and is involved in regulation of T cell activation. *J. Exp. Med.* **2000**, *191*, 1591–1604.
- (8) Nada, S.; Yagi, T.; Takeda, H.; Tokunaga, T.; Nakagawa, H.; Ikawa, Y.; Okada, M.; Aizawa, S. Constitutive activation of Src family kinases in mouse embryos that lack Csk. *Cell* **1993**, *73*, 1125–1135.
- (9) Talamonti, M. S.; Roh, M. S.; Curley, S. A.; Gallick, G. E. Increase in activity and level of pp60c-src in progressive stages of human colorectal cancer. *J. Clin. Investig.* **1993**, *91*, 53–60.
- (10) Ogawa, A.; Takayama, Y.; Sakai, H.; Chong, K. T.; Takeuchi, S.; Nakagawa, A.; Nada, S.; Okada, M.; Tsukihara, T. Structure of the carboxyl-terminal Src kinase, Csk. *J. Biol. Chem.* **2002**, 277, 14351–14354.
- (11) Jamros, M. A.; Oliveira, L. C.; Whitford, P. C.; Onuchic, J. N.; Adams, J. A.; Blumenthal, D. K.; Jennings, P. A. Proteins at work: A combined small angle x-ray scattering and theoretical determination of the multiple structures involved on the protein kinase functional landscape. *J. Biol. Chem.* **2010**, 285, 36121–36128.
- (12) Jamros, M. A.; Oliveira, L. C.; Whitford, P. C.; Onuchic, J. N.; Adams, J. A.; Jennings, P. A. Substrate-Specific Reorganization of the Conformational Ensemble of CSK Implicates Novel Modes of Kinase Function. *PLoS Comput. Biol.* **2012**, *8*, e1002695.
- (13) Lieser, S. A.; Shaffer, J.; Adams, J. A. Src tail phosphorylation is limited by structural changes in the regulatory tyrosine kinase Csk. *J. Biol. Chem.* **2006**, *281*, 38004–38012.
- (14) Sun, G.; Budde, R. J. Mutations in the N-terminal regulatory region reduce the catalytic activity of Csk, but do not affect its recognition of Src. *Arch. Biochem.* **1999**, 367, 167–172.
- (15) Wong, L.; Lieser, S.; Chie-Leon, B.; Miyashita, O.; Aubol, B.; Shaffer, J.; Onuchic, J. N.; Jennings, P. A.; Woods, V. L.; Adams, J. A. Dynamic coupling between the SH2 domain and active site of the COOH terminal Src kinase, Csk. J. Mol. Biol. 2004, 341, 93–106.
- (16) Shekhtman, A.; Ghose, R.; Wang, D.; Cole, P. A.; Cowburn, D. Novel mechanism of regulation of the non-receptor protein tyrosine kinase Csk: Insights from NMR mapping studies and site-directed mutagenesis. *J. Mol. Biol.* **2001**, *314*, 129–138.
- (17) Cole, P. A.; Shen, K.; Qiao, Y.; Wang, D. Protein tyrosine kinases Src and Csk: A tail's tale. *Curr. Opin. Chem. Biol.* **2003**, *7*, 580–585.
- (18) Lamers, M. B.; Antson, A. A.; Hubbard, R. E.; Scott, R. K.; Williams, D. H. Structure of the protein tyrosine kinase domain of C-

- terminal Src kinase (CSK) in complex with staurosporine. *J. Mol. Biol.* **1999**, 285, 713–725.
- (19) Shaffer, J.; Sun, G.; Adams, J. A. Nucleotide release and associated conformational changes regulate function in the COOH-terminal Src kinase, Csk. *Biochem.* **2001**, *40*, 11149–11155.
- (20) Songyang, Z.; Shoelson, S. E.; McGlade, J.; Olivier, P.; Pawson, T.; Bustelo, X. R.; Barbacid, M.; Sabe, H.; Hanafusa, H.; Yi, T. Specific motifs recognized by the SH2 domains of Csk, 3BP2, fps/fes, GRB-2, HCP, SHC, Syk, and Vav. Mol. Cell. Biol. 1994, 14, 2777–2785.
- (21) Ghose, R.; Shekhtman, A.; Goger, M. J.; Ji, H.; Cowburn, D. A novel, specific interaction involving the Csk SH3 domain and its natural ligand. *Nat. Struct. Biol.* **2001**, *8*, 998–1004.
- (22) Sondhi, D.; Cole, P. A. Domain interactions in protein tyrosine kinase Csk. *Biochem* **1999**, *38*, 11147–11155.
- (23) Barkho, S.; Pierce, L. C.; Li, S.; Adams, J. A.; Jennings, P. A. Theoretical insights reveal novel motions in Csk's SH3 domain that control kinase activation. *PLoS One* **2015**, *10*, e0127724.
- (24) Lin, X.; Ayrapetov, M. K.; Lee, S.; Parang, K.; Sun, G. Probing the communication between the regulatory and catalytic domains of a protein tyrosine kinase, Csk. *Biochem.* **2005**, *44*, 1561–1567.
- (25) Mills, J. E.; Whitford, P. C.; Shaffer, J.; Onuchic, J. N.; Adams, J. A.; Jennings, P. A. A novel disulfide bond in the SH2 Domain of the C-terminal Src kinase controls catalytic activity. *J. Mol. Biol.* **2007**, *365*, 1460–8
- (26) Chahine, J.; Cheung, M. S. Computational studies of the reversible domain swapping of p13suc1. *Biophys. J.* **2005**, 89, 2693–2700.
- (27) Gosavi, S.; Chavez, L. L.; Jennings, P. A.; Onuchic, J. N. Topological frustration and the folding of interleukin-1 β . *J. Mol. Biol.* **2006**, 357, 986–996.
- (28) Oliveira, L. C.; Schug, A.; Onuchic, J. N. Geometrical features of the protein folding mechanism are a robust property of the energy landscape: A detailed investigation of several reduced models. *J. Phys. Chem. B* **2008**, *112*, 6131–6136.
- (29) Noel, J. K.; Chahine, J.; Leite, V. B.; Whitford, P. C. Capturing Transition Paths and Transition States for Conformational Rearrangements in the Ribosome. *Biophys. J.* **2014**, *107*, 2881–2890.
- (30) Cota, J.; Oliveira, L. C.; Damasio, A. R.L.; Citadini, A. P.; Hoffmam, Z. B.; Alvarez, T. M.; Codima, C. A.; Leite, V. B.P.; Pastore, G.; de Oliveira-Neto, M.; Murakami, M. T.; Ruller, R.; Squina, F. M. Assembling a xylanase-lichenase chimera through all-atom molecular dynamics simulations. *Biochim. Biophys. Acta* **2013**, *1834*, 1492–1500.
- (31) de Oliveira, L. C.; da Silva, V. M.; Colussi, F.; Cabral, A. D.; de Oliveira Neto, M.; Squina, F. M.; Garcia, W. Conformational Changes in a Hyperthermostable Glycoside Hydrolase: Enzymatic Activity Is a Consequence of the Loop Dynamics and Protonation Balance. *PloS one* **2015**, *10*, No. e0118225.
- (32) Clementi, C.; Nymeyer, H.; Onuchic, J. N. Topological and energetic factors: What determines the structural details of the transition state ensemble and 'en-route' intermediates for protein folding? An investigation for small globular proteins. *J. Mol. Biol.* **2000**, 298, 937–953.
- (33) Noel, J. K.; Whitford, P. C.; Onuchic, J. N. The shadow map: A general contact definition for capturing the dynamics of biomolecular folding and function. *J. Phys. Chem. B* **2012**, *116*, 8692–8702.
- (34) Whitford, P. C.; Noel, J. K.; Gosavi, S.; Schug, A.; Sanbonmatsu, K. Y.; Onuchic, J. N. An all-atom structure-based potential for proteins: bridging minimal models with all-atom empirical forcefields. *Proteins: Struct. Funct. Genet.* **2009**, *75*, 430–441.
- (35) Jackal is supported by funding from the National Science Foundation and National Institutes of Health Grant # DBI-9904841 and 5 R37 GM30518; http://honig.c2b2.columbia.edu/jackal.
- (36) Noel, J. K.; Levi, M.; Raghunathan, M.; Lammert, H.; Hayes, R. L.; Onuchic, J. N.; Whitford, P. C. SMOG 2: A Versatile Software Package for Generating Structure-Based Models. *PLoS Comput. Biol.* **2016**, *12*, e1004794.
- (37) Hess, B.; Kutzner, C.; Van Der Spoel, D.; Lindahl, E. GROMACS 4: Algorithms for highly efficient, load-balanced, and scalable molecular simulation. *J. Chem. Theory Comput.* **2008**, *4*, 435–447.

- (38) Berendsen, H. J.; Postma, J. P.; Van Gunsteren, W. F.; Dinola, A.; Haak, J. R. Molecular dynamics with coupling to an external bath. *Chem. Phys.* **1984**, *81*, 3684–3690.
- (39) Swendsen, R. H. Modern methods of analyzing Monte Carlo computer simulations. *Phys. A: Stat. Mech. Appl.* **1993**, *194*, 53–62.
- (40) Levinson, N. M.; Seeliger, M. A.; Cole, P. A.; Kuriyan, J. Structural Basis for the Recognition of c-Src by Its Inactivator Csk. *Cell* **2008**, *134*, 124–134.
- (41) Russell, R. B.; Barton, G. J. Multiple protein sequence alignment from tertiary structure comparison: Assignment of global and residue confidence levels. *Proteins: Struct. Funct. Genet.* **1992**, *14*, 309–323.
- (42) MacKerell, A. D., Jr; Bashford, D.; Bellott, M.; Dunbrack, R. L., Jr; Evanseck, J. D.; Field, M. J.; Fischer, S.; Gao, J.; Guo, H.; Ha, S.; et al. All-Atom Empirical Potential for Molecular Modeling and Dynamics Studies of Proteins. *J. Phys. Chem. B* **1998**, *102*, 3586–3616.
- (43) Zoete, V.; Cuendet, M. A.; Grosdidier, A.; Michielin, O. SwissParam: A fast force field generation tool for small organic molecules. *J. Comput. Chem.* **2011**, 32, 2359–2368.
- (44) Parrinello, M.; Rahman, A. Polymorphic transitions in single crystals: A new molecular dynamics method. *J. Appl. Phys.* **1981**, *52*, 7182–7190.
- (45) Berendsen, H. J.; van der Spoel, D.; van Drunen, R. GROMACS: A message-passing parallel molecular dynamics implementation. *Comput. Phys. Commun.* **1995**, *91*, 43–56.
- (46) Hess, B.; Bekker, H.; Berendsen, H. J.; Fraaije, J. G. LINCS: A Linear Constraint Solver for molecular simulations. *J. Comput. Chem.* 1997, 18, 1463–1472.
- (47) Huang, H.; Zhao, R.; Dickson, B. M.; Skeel, R. D.; Post, C. B. α C helix as a switch in the conformational transition of Src/CDK-like kinase domains. *J. Phys. Chem. B* **2012**, *116*, 4465–4475.
- (48) Wong, L.; Lieser, S. A.; Miyashita, O.; Miller, M.; Tasken, K.; Onuchic, J. N.; Adams, J. A.; Woods, V. L.; Jennings, P. A. Coupled motions in the SH2 and kinase domains of Csk control Src phosphorylation. *J. Mol. Biol.* **2005**, *351*, 131–143.
- (49) Onuchic, J. N.; Kobayashi, C.; Miyashita, O.; Jennings, P.; Baldridge, K. K. Exploring biomolecular machines: Energy landscape control of biological reactions. *Philos. Trans. R. Soc. London B: Biol. Sci.* **2006**, *361*, 1439–1443.
- (50) Kinoshita, T.; Matsubara, M.; Ishiguro, H.; Okita, K.; Tada, T. Structure of human Fyn kinase domain complexed with staurosporine. *Biochem. Biophys. Res. Commun.* **2006**, 346, 840–844.